Proceedings of the XVII ECSMGE-2019
Geotechnical Engineering foundation of the future
ISBN 978-9935-9436-1-3

doi: 10.32075/17ECSMGE-2019-0043

XVII European Conference
ECSMGE 2019
Reykjavik
on Soil Mechanics
and Geotechnical Engineering

Design of draining cores to control seepage through embankment dams

Projet des zones de drainage pour contrôle les infiltrations dans les barrages en terre

Francesco Federico
Associate Professor of Geotechnics, University of Rome Tor Vergata (Rome, Italy)

Ruggiero Jappelli
Past Professor of Geotechnics, University of Rome Tor Vergata (Rome, Italy)

Chiara Cesali
Ph. D. Student in Geotechnical Engineering, University of Rome Tor Vergata (Rome, Italy)

ABSTRACT: Watertightness of embankment dams can be ensured by an impervious facing covering the upstream slope, or by a silty or clayey core. In the first case, especially in seismic zones, the remote circumstance must be conveniently considered that the facing and the embankment upstream shell severely crack and become wholly ineffective.
To face this undesired situation, a draining core, made of cohesionless self-protected material, allowing a full control of the seepage process, can be provided. The core characteristics (geometry, properties and granulometric stability of materials,..), must be carefully designed through advanced numerical analyses, including seepage flow and "*granulometric stability*", under critical hydraulic conditions, as proposed in the paper.
According to this procedure, the characteristics (geometry, properties) of materials composing a zoned embankment dam in South Italy, endowed with an upstream impervious bituminous facing and a central draining zone, are back-analyzed.

RÉSUMÉ: L'étanchéité des barrages en remblais peut être garantie par un revêtement imperméable recouvrant la pente en amont, ou par un noyau limoneux ou argileux. Dans le premier cas, en particulier dans les zones sismiques, il faut également tenir compte de la circonstance éloignée selon laquelle le revêtement et le remblai en amont se fissurent et deviennent totalement inefficaces.
Pour faire face à cette situation indésirable, un noyau drainant en matériau auto-protégé sans cohésion, permettant un contrôle total du processus de écoulement, peut être prévu.
Les caractéristiques essentielles (géométrie, propriétés et stabilité granulométrique des matériaux, ..) peuvent être soigneusement définies selon une procédure avancée, comprenant des analyses numériques du débit de écoulement ainsi que la «stabilité granulométrique», dans les conditions hydrauliques critiques proposées dans le memoire. Selon cette procédure, les caractéristiques (géométrie, propriétés) des matériaux composant un barrage zoné dans le sud de l'Italie, revêtu d'un revêtement bitumineux imperméable en amont et d'une zone de drainage centrale, sont rétrospectées.

Keywords: Embankment dams, Design criteria, Central draining core, Seepage flow analyses, Seismic conditions.

1 CONTROL OF SEEPAGE FLOW UNDER CRITICAL CONDITIONS

Embankment dams can be generally distinguished in two fundamental types: *i) homogeneous,* with an impervious facing covering the upstream slope; *ii) zoned,* with an outer shell usually of a sandy material and an inner core of impervious silty or clayey soils. The choice of the type depends on site topography (e.g. narrow or wide stream valley, depth of soil overlying bedrock, spillway capacity), foundation (e.g. tendency for large settlements, prevention of piping, excessive seepage losses), available materials, environmental and economic considerations (e.g. seismic activity).

In order to use the materials obtained from site excavations, a homogeneous embankment with an upstream impervious facing is preliminary considered (Figure 1a).

Undesired situations possibly related to the structural failure of the upstream facing, especially in seismic zones, might however follow this simple solution (Jappelli et al 1988).

As safeguarding measure to control the seepage flow, a drainage system under the bituminous facing or within the embankment (e.g. vertical/chimney central drain and horizontal drain up to the downsteam toe) is generally adopted (Figure 1b).

However, these thin drainage layers could not be able to support high stresses deriving from an earthquake and could be susceptible to the dangerous effects of particle migration phenomena, inducing variations in permeability coefficient (Federico and Montanaro 2011, Federico and Cesali 2018).

A possible solution consists in a pervious central large core and a drainage conduit to convey downstream the seepage discharge (Figure 2a). This solution is not even fully satisfactory because the safety of dam depends on the efficiency of a single drainage element (the conduit). A downstream more pervious shell acting as a drain easily controlling the flow lines could be adopted (Figure 2b).

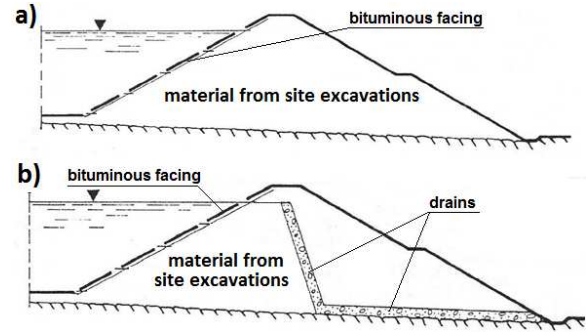

Figure 1. a) Homogeneous dam with upstream facing; b) Dam with drainage systems.

According to this last configuration (Figure 2b), the safety of the dam is ensured by the upstream bituminous facing and by the progressive change in the zonation of the embankment, controlling the seepage flow, should damages or failures of the upstream facing coupled with widespread cracks within the upstream material occur under critical (or seismic) conditions (Jappelli et al. 1988).

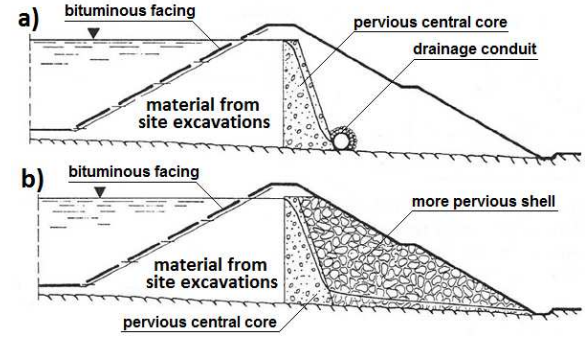

Figure 2. Dam with a) pervious central core and drainage conduit; b) progressive change in the zonation, from the upstream to downstream.

2 PROPOSED PROCEDURE TO DESIGN DRAINING CORES

To design a zonation fully controlling the seepage flow in embankment dams endowed by an upstream bituminous facing, under critical conditions (Figure 2b), an original analysis

procedure has been developed and proposed (Jappelli et al. 1998). The following steps are planned.

1) *Seepage numerical analyses* in unsteady and steady conditions, under different hypotheses for core thickness (L_c) and construction materials.

The simulations aim to search for *i)* interstitial pressures, piezometric heads and free surface profile in order to identify the zones affected by high hydraulic gradients and *ii)* the *exit point* elevation at the contact "*core - downstream material"*, corresponding to the condition the free surface reaches the downstream toe (Figure 3). On account that the upstream facing could be affected by cracks under critical (seismic) conditions and could not be able to exhibit appreciable resistance to seepage water, the hydraulic resistance opposed by the facing and the upstream shell are cautiously neglected.

2) *Definition of the thickness* (L_c) of the draining core on the basis of its *critical filling time*.

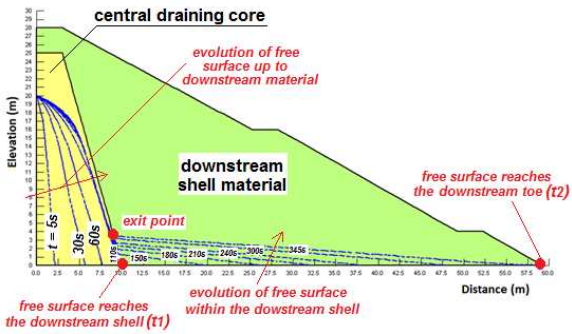

Figure 3. Definition of critical times.

The *critical times* taken by the free surface to *(a)* cross the central core and reach the downstream shell (t_1), and *(b)* approach the steady state condition at the downstream toe (t_2), at an elevation of the *exit point* defined in Figure 3, are determined.

3) *Evaluation of the granulometric stability* *i)* internally to the core material (*suffusion*); *ii)* at the contact between the core and the dowstream shell materials (*contact erosion*), under the maximum hydraulic gradient.

The grain size distribution of the core material is chosen according to its susceptibility to particle migration; the phenomenon can be verified by first applying the empirical criteria (e.g. Sherard and Dunnigan 1985, Wan and Fell 2004) and then the available advanced numerical models (e.g. Indraratna and Vafai 1997). Among these, the numerical procedure proposed by Federico and Montanaro (2011), may be applied allowing to take into account simultaneously seepage flow (1D) and particle migration, i.e. the coupled effects of the geometrical (voids volume distribution, porosity) and hydraulic (local hydraulic gradient, seepage flow velocity, permeability) properties.

To this purpose, the system composed by two contacting different materials (*B-T*) is divided into several elements (Figure 4), each characterized by appropriate values of initial grain size distribution (GSD), porosity (n) and permeability (k).

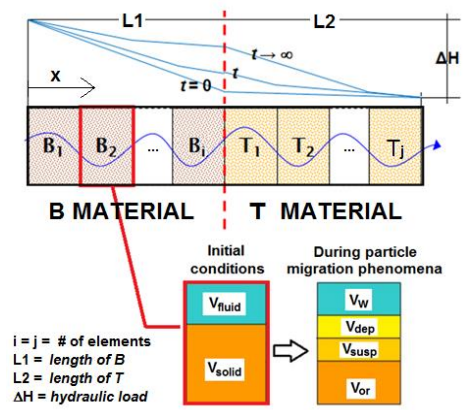

Figure 4. Numerical procedure to simulate particle migration phenomena: problem's setting.

Each element is schematically composed by *original* (not eroded) material (V_{or}), *deposited* particles (V_{dep}) and *suspended* particles (V_{susp}) due to erosion/deposition associated with migration and water saturation of the *i-th* element (V_w). The variables *GSD, n, k* evolve because of erosion/deposition processes,

governed by geometrical-probabilistic laws allowing to take into account the volume voids (VVD) and constriction size distribution (CSD) under the hydraulic boundary conditions.

2.1 Application

The proposed procedure has been sistematically applied to different configurations. The seepage flow analyses (SEEP/W FE code) were carried out by considering: *i)* the curves of the volumetric water content (VWC), for the central draining core material, shown in Figure 5: curve *a)* is typical of a coarse grained material, affected by low capillarity; curve *b)* is typical of finer grained material, characterized by a non-negligible capillarity; *ii)* $k = 10^{-2}$ and 10^{-3} cm/s for the central draining core, and $k = 1$ cm/s for the downstream shell material; *iii)* draining core thickness $L_c = 5 \div 50$ m; *iv)* hydraulic load $H =$ 10, 15, 20, 25, 30 m.

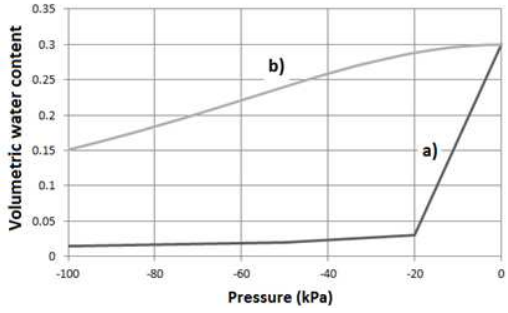

Figure 5. The two curves of the volumetric water content (VWC) considered in the analyses.

For all simulations, the corresponding critical time t_1 taken by the free surface to cross the central core and reach the downstream shell is determined. Some of the obtained results in term of *core thickness vs critical time*, for different values of pemeability of the draining core and hydraulic gradient, are shown in the Figures 6 and 7. Referring to the "*internal stability*" of granular materials, the numerical procedure (Federico and Montanaro 2011) has been aimed at *verifying* some *speditive* empirical criteria (e.g. Wan and Fell 2004).

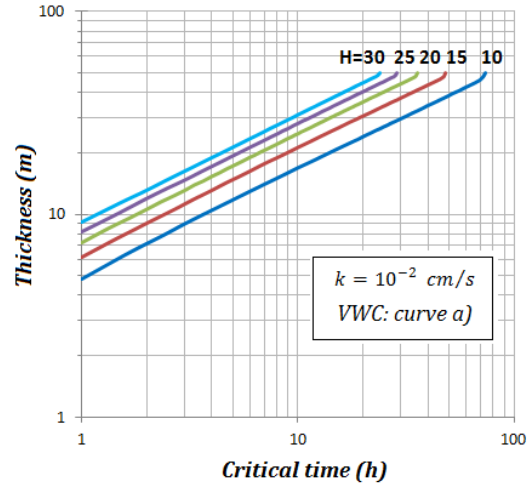

Figure 6. Core thickness vs critical time, t_1 (VWC from curve a, Fig.5); $k = 10^{-2}$ cm/s for draining core).

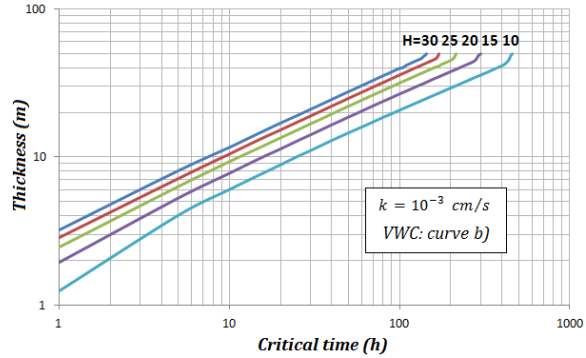

Figure 7. Core thickness vs critical time, t_1 (VWC from curve b, Fig.5); $k = 10^{-3}$ cm/s for draining core).

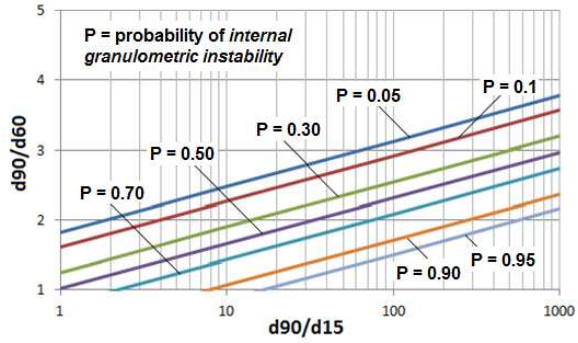

Figure 8. Probability of internal instability for soils composed by gravel, sand, silt and low clay content (d90 = diameter of fine soil corresponding to 90% of the passing percentage by weight; d60, d15 = diameters of coarse soil corresponding to 60% and 15% of the passing percentage by weight).

The results, summarized in Figure 8, confirm the experimental observations, on which the considered empirical critieria were developed.

The above graphs may be used to the first hand design of a central draining core.

3 THE CASE STUDY OF ANAPO PUMPED-STORAGE POWER PLANT

The plant consists of *i)* an *upper reservoir* of $5.6 \cdot 10^6 m^3$ volume located in Sicily on a plateau of the Climiti Mountains, which forms part of the left side of the Anapo river drainage basin; *ii)* two *steel penstocks,* each with a diameter of 4.40 m and length of 520 m; *iii)* an *underground powerhouse* equipped with four equal reversible turbine-generator units; *iv)* two *discharge tunnels,* each with a diameter of 5.50 m and length of 700 m; *v)* a *lower reservoir* with a capacity of $7.3 \cdot 10^6$ m^3, located on one bank of the Anapo river whose course has been reshaped by means of a diversion channel.

The waterproofing structure consists of an impervious facing of bituminous concrete.

The territory is considered as a medium-high seismic zone (according to national seismic regulations), due to the proximity to Cosimo's fault (Jappelli et al. 1988).

The design of the embankment dams has been directed to ensure adequate safety with a fully achieved control of the stored water even in the remote event that the upstream facing suddenly becomes ineffective under seismic conditions.

Both embankments are composed (Figure 9) by: upstream shell (A), built with materials obtained from site excavations; central core (B), composed by material from a quarry of limestone rocks; downstream shell (B1), by material from a limestone quarry for the upper reservoir and basalts for the lower reservoir. The core thickness (B) is 10 m length, at the base, and 3 m at the crest. The permeability coefficient has been obtained through lab tests, according to dry unit weight of the materials (Figure 9).

Particularly, the permeability (k) of the zone A, for the lower and the upper embankments ranges between $10^{-6} \div 5 \cdot 10^{-4}\ cm/s$ and $3 \cdot 10^{-4} \div 3 \cdot 10^{-3}\ cm/s$, respectively; the permeability of the zone B is $10^{-2} \div 10^{-1}\ cm/s$; for the downstream shell (B1), k assumes higher values than $10^{-1}\ cm/s$ and $1\ cm/s$, for the lower and upper embankments, respectively (Jappelli et al. 1988).

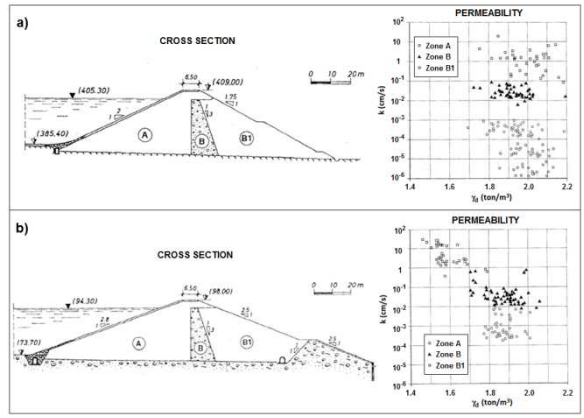

Figure 9. Cross sections and permeability of materials of the a) lower and b) upper embankmemts of Anapo pumped-storage power plant (Sicily, Italy).

3.1 Seepage flow analyses

The evolution of the free surface profile (SEEP/W FE code) through the central core and the downstream shell of the lower embankment is shown in Figure 10.

The critical time (t_1) is approximately equal to 2 hours and the water takes about 4 hours (t_2) to cross the downstream material. The steady state conditions reached at the end of the process are shown in Figures 11, 12, 13.

The piezometric head coupled to the velocity vectors, the interstitial pressure and the hydraulic gradient allow to identify the zones affected by high hydraulic gradients, more likely susceptible to internal erosion phenomena.

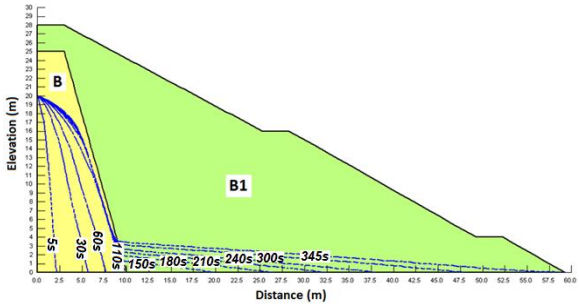

Figure 10. Evolution of the free surface profile (unsteady state conditions).

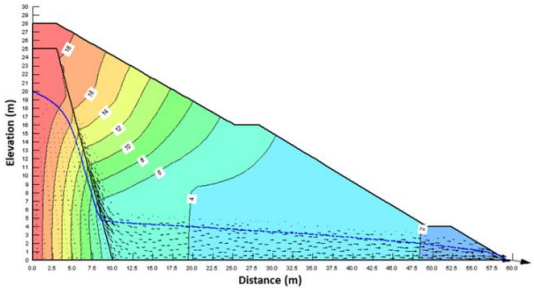

Figure 11. Distribution of piezometric head, velocity vectors and free surface profile (steady state).

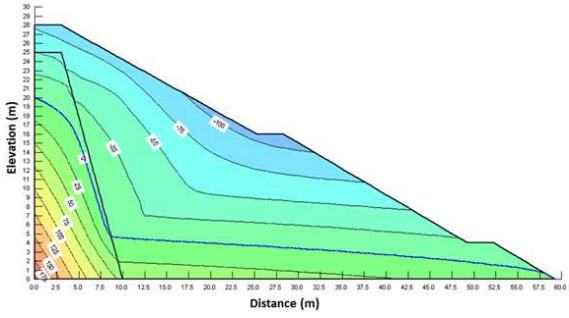

Figure 12. Distribution of interstitial pressure and free surface profile (steady state).

Within these zones, the hydraulic head along the abscissa x (Figure 13) is the input of the analysis of particle migration process which was carried out with the described numerical procedure (Federico and Montanaro 2011, Federico and Cesali 2018). Obviously, the piezometric head is lost, in large amount, in the central core, ΔH_B = 15.5 m, where permeability is lower than the permeability of the B1 material. The average hydraulic gradient acting on the central core is $i_{x,medium,B}$ = 1.55; in the downstream shell (60 m long) the piezometric head is ΔH_{B1} = 4.5 m and the average hydraulic gradient is $i_{xmedium,B1}$ = 0.075. The zone affected by the highest gradient, i_x = 2.2, is highlighted with a black circle in Figure 13.

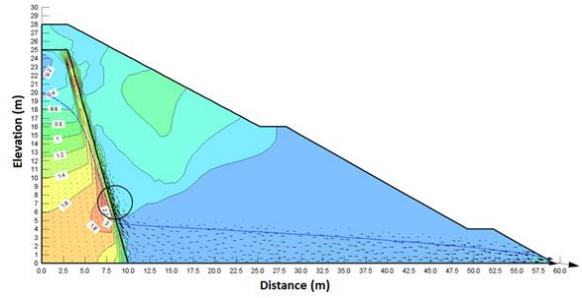

Figure 13. Distribution of hydraulic gradient (steady state) and detection of the zone more likely susceptible to particles migration.

3.2 Particle migration analyses

Particle migration possibly occurs at the contact between the central core (*B*) and the downstream shell (*B1*), especially for high hydraulic gradients (Federico and Montanaro 2011, Federico and Cesali 2018).

The vulnerability of the materials, through the comparison of the grain size distribution (GSD) with the volume voids (VVD) or constriction size distribution (CSD) must be preliminarily evalutated. Referring to Figure 14, the lower GSD curve of *B* and the GSD of *B1* both fulfill Terzaghi's criteria (i.e. $4d_{B,15} < d_{B1,15} < 4d_{B,85}$), with respect to the upper GSD of *B*. The CSD curves of lower GSD of *B* and *B1* intersect the upper GSD curve of the central core (*B*) for *P* (Passing) = 25% and 55%, respectively.

Then, the particles smaller than the diameter (*d*) corresponding to *P* = 25% (e.g. 2 mm, lower GSD of *B*) and 55% (e.g. 13 mm, *B1*), could be eroded, causing an increase of the permeability and possible failure due to internal erosion.

To better understand the *microscopic behaviour* of the materials, the described numerical procedure (Federico and Montanaro 2011) has been applied.

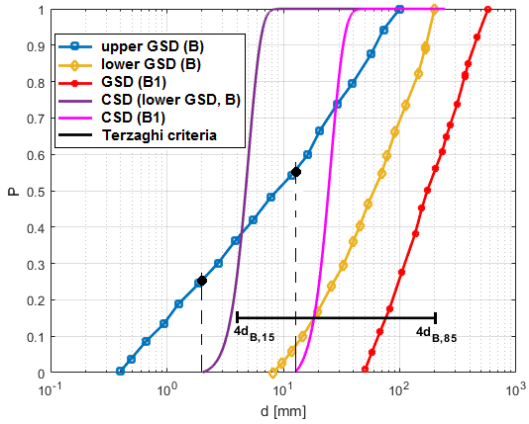

Figure 14. GSD and CSD curves of B and B1 materials: passing (P) vs diameter (d).

The following input parameters (see Figure 4) are assigned: $i = j = 4$ (number of elements for both materials of the *B-T* system; L_1 = 1.2 m; L_2 = 3.4 m; $\Delta H_{B\text{-}T}$ = 3.5 m.

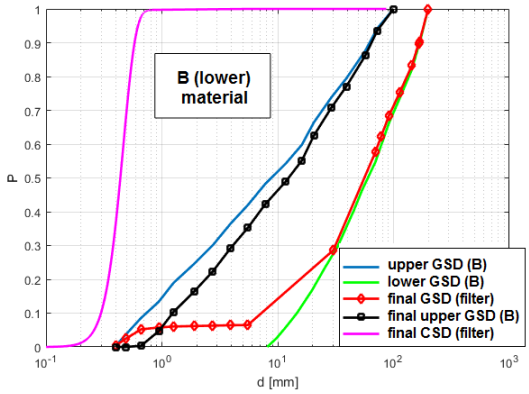

Figure 15. Computed GSD and CSD curves of the natural filter, for upper and lower GSDs of B.

For both materials (lower GSD of *B* and *B1*), the formation of a "*natural filter*" (red curves), affected by granulometric properties intermediate between the upper and lower GSDs of *B* (Figure 15) and between *B* (upper GSD) and *B1* (Figure 16), is observed. In *B(lower)-B(upper)* system (Figure 17a), the maximum diameter of the eroded particles and the thickness of the *natural filter* (Figure 17b) are smaller than in the *B(upper)-B1* system. The *B(upper)* particle migration stabilizes after approximately 0.5 hours, in *B(lower)-B(upper)* system; in the *B(upper)-B1*, after 2 hours, it happens that particles of *B(upper)* affected by the diameter $d_{B,35}$ are still susceptible to erosion (Figure 17a).

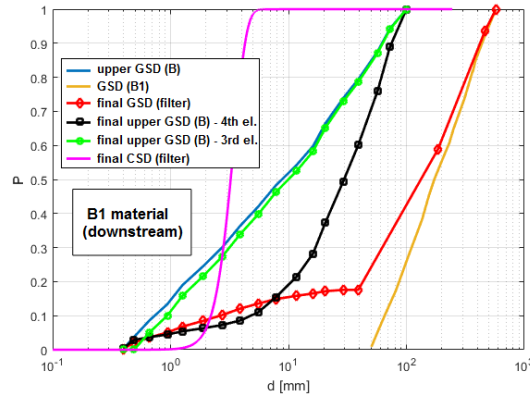

Figure 16. Computed GSD and CSD curves of the natural filter, for upper GSD of B and B1 material.

The particles affected by $d_{B,15}$ travel from the *B(upper)-B1* interface, within *B1*, a distance (e.g. 12.5 cm) farther than that one travelled (e.g. 1.6 cm) within *B(lower)* material (Figure 17b).

The above described analyses show that, at the *micro scale*, the process within the two systems may evolve differently; the '*complete*' formation of *natural filter* in *B(upper)-B1* is slower than *B(lower)-B(upper)*; so the last system becomes able to arrest the migration of $d_{B,15}$ particles after about 2.5 hours, approximately.

4 CONCLUDING REMARKS

Intense seismicity and high erodibility of available embankment construction materials at dam sites often complicate design problems. The effects of very strong earthquakes may be mitigated by providing an embankment dam (endowed by an upstream facing) with a large central core of a cohesionless self-healing material. This material maintains its structural integrity even under the severe strains resulting from cyclic actions.

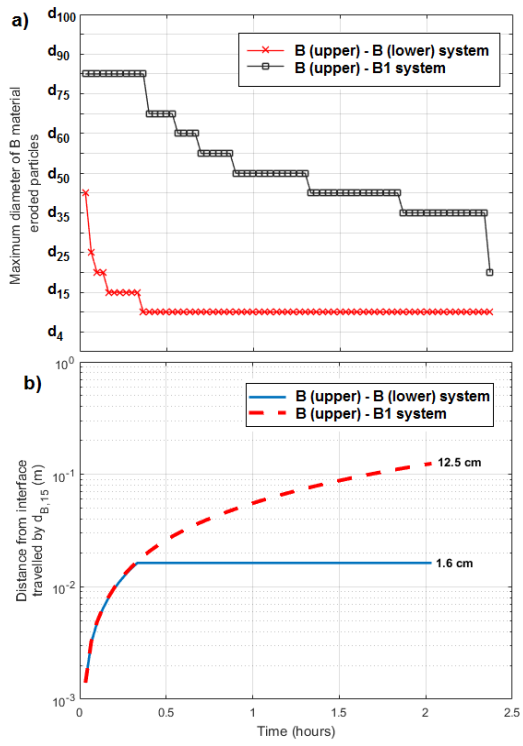

Figure 17. a) Maximum diameter of material B (upper) eroded particles vs time; b) Distance from materials interface travelled by $d_{B,15}$.

Zonation controls the relevant transient seepage flow occurring through the core; in turn, this last flow is controlled by a downstream shell of a more pervious material.

The internal erosion of the central draining core material as well as the clogging of pores of the downstream shell require carefull analyses. The proposed design procedure allows also to ensure the compatibility of contacts between different materials under hydraulic gradients possibly prevailing in critical transient flow conditions. Referring to the embankment dams of the analyzed pumped-storage plant, endowed with bituminous facing and large central draining cores, the effects of core thickness and materials properties on the evolution of potential seepage flow processes through the dams have been investigated in the event of catastrofic failure of the impervious face and extensive cracking of the upstream material. Results of FEM simulation ensure that t_1 = 2 hours would elapse before the free surface reach the downstream shell (unsteady state) and approach the steady state condition or reach the downstream toe characterized by a critical elevation of the *exit point* (t_2 = 4 hours), according to a controlled delay of the discharge flow. Advanced analyses of potential particle migration confirm the granulometric stability at the contact between the core materials and the downstream shell, even in the most adverse hydraulic conditions, considered in the paper.

5 REFERENCES

Jappelli, R., et al. (1988). "Impervious facing and large central drain for the embankment dams of a pumped-storage plant". *XVI ICOLD, Q61, S. Francisco,1988.*

Federico, F., Montanaro, A. (2011). "Granulometric stability of moraine embankment dam materials. Theoretical procedure and back-analysys of cases". *6th Int. Conf. on Dam Engin., Lisbon, Portugal.*

Federico, F., Cesali, C. (2018). "A numerical procedure to simulate particles migration at the contact between different materials in earthfill dams". *26th Annual Meeting of EWG on Internal Erosion, Milano, Settembre 2018.*

Indraratna, B., Vafai, F. (1997). Analytical model for particle migration within base soil-filter system. *J. of Geotechnical and Geoenvir. Engineering*, vol. 123, pp. 100-109.

Sherard, J.L., Dunnigan, L.P. (1985). "Filters and leakage control in embankment dams". *Seepage and Leakage from dams and Impoundments, ASCE, NY*, 1-29.

Wan, C.F., Fell, R. (2004). "Investigation of internal erosion by the process of suffusion in embankment dams and their foundations". *Internal Erosion of Dams and their Foundations - Fell & Fry (eds), Taylor & Francis Group, London, ISBN 978-0-415.*